J. Membrane Biol. 178, 195–204 (2000)
DOI: 10.1007/s002320010027

The Journal of
Membrane
Biology

Activation of Metabotropic Glutamate Receptors Inhibits Synapsin I Phosphorylation in Visceral Sensory Neurons

M. Hay, C.J. Hoang, E.M. Hasser, E.M. Price
Dalton Cardiovascular Research Center, Department of Veterinary Biomedical Sciences, University of Missouri, Columbia, MO 65255, USA

Received 28 June 2000/Revised: 11 September 2000

Abstract. Activation of glutamate metabotropic receptors (mGluRs) in nodose ganglia neurons has previously been shown to inhibit voltage-gated Ca^{++} currents and synaptic vesicle exocytosis. The present study describes the effects of mGluRs on depolarization-induced phosphorylation of the synaptic-vesicle-associated protein synapsin I. Depolarization of cultured nodose ganglia neurons with 60 mM KCl resulted in an increase in synapsin I phosphorylation. Application of mGluR agonists 1-aminocyclopentane-1s-3r-dicarboxylic acid (t-ACPD) and L(+)-2-Amino-4-phosphonobutyric acid (L-AP4) either in combination or independently inhibited the depolarization induced phosphorylation of synapsin I. Application of the mGluR antagonist (RS)-α-Methyl-4-carboxyphenylglycine (MCPG) blocked t-ACPD-induced inhibition of synapsin phosphorylation but not the effects of L-AP4. In addition, application of either t-ACPD or L-AP4 in the absence of KCl induced depolarization had no effect on resting synapsin I phosphorylation. RT-PCR analysis of mGluR subtypes in these nodose ganglia neurons revealed that these cells only express group III mGluR subtypes 7 and 8. These results suggest that activation of mGluRs modulates depolarization-induced synapsin I phosphorylation via activation of mGluR7 and/or mGluR8 and that this process may be involved in mGluR inhibition of synaptic vesicle exocytosis in visceral sensory neurons of the nodose ganglia.

Key words: Synaptic proteins — mGluRs — Nodose ganglia — Baroreceptors — Synapsin — Synaptic transmission

Introduction

Identification of the mechanisms regulating neuronal transmission is central to the understanding of the physiological and pathophysiological modulation of central nervous system function. Metabotropic glutamate receptors (mGluRs) are a heterogeneous class of G-protein-coupled receptors known to be important in glutamate neurotransmission [4]. Activation of presynaptic mGluRs have been suggested to modulate synaptic transmission and to inhibit the release of neurotransmitters in a number of different neuronal cell types. While the mechanisms underlying these effects of mGluRs on synaptic transmission are still unknown, it has been hypothesized that activation of these receptors may inhibit voltage-gated calcium channels and synaptic protein phosphorylation, both of which are critical for effective neurotransmission [4, 15].

The nucleus of the solitary tract (NTS) receives visceral afferent input via sensory neurons whose cell bodies are located in the nodose ganglia. Activation of mGluRs in the NTS have been shown to presynaptically inhibit solitary tract and baroreceptor-evoked NTS responses through an undetermined mGluR subtype [8, 9]. Whole-cell patch-clamp studies from nodose ganglia neurons have shown that activation of mGluRs inhibits the activity of the N-type voltage-gated Ca^{++} channels [16]. Furthermore, activation of L-AP4-sensitive mGluRs has been found to inhibit synaptic vesicle exocytosis in visualized boutons from nodose ganglia and baroreceptor neuronal terminals in culture [15].

Synaptic protein phosphorylation plays an important role in the regulation of neuronal synaptic transmission [12, 18, 23, 25]. Synapsins, which represent the most abundant protein in synaptic vesicles, are a family of synaptic proteins that have been suggested to be important in sustaining synaptic transmission [11, 28]. Synapsin I has a high affinity for the synaptic vesicle membrane and possesses specific domains which facilitate crosslinking of synaptic vesicles to the actin cytoskeleton in the nerve terminal [12, 13]. The phosphorylation state of synapsin I is increased by factors that increase Ca^{++}-

Correspondence to: M. Hay

dependent exocytosis such as action potential generation, high potassium-induced depolarization and veratridine. Phosphorylation of synapsin I by Ca^{++}/calmodulin-dependent kinase (CaM kinase II) or cAMP-dependent protein kinase occurs during increased neuronal activity and results in a decrease in the affinity of synapsin I for the synaptic vesicle membrane. Further, the phosphorylation of synapsin I has been shown to potentiate the release of neurotransmitter [3, 28].

Since mGluR agonists inhibit visceral sensory neuronal voltage-gated Ca^{++} channels and synaptic vesicle exocytosis, we hypothesized that activation of mGluRs may regulate synapsin I phosphorylation. The purpose of this study was to determine the effects of mGluR activation on resting and depolarization-induced increases in synapsin I phosphorylation in nodose ganglia neurons. Our results clearly demonstrate that mGluR activation inhibits depolarization-induced synapsin I phosphorylation in visceral sensory neurons. This attenuation of synapsin I phosphorylation is consistent with the inhibition of synaptic vesicle exocytosis observed during activation of mGluR receptors.

Materials and Methods

Cell Culture

Nodose neurons were isolated and cultured as described previously [15, 20]. Briefly, nodose ganglia from 18–21-day-old Sprague-Dawley rats were isolated and collected in cold Neuron Complete Medium (NCM) containing Eagle's Minimum Essential Medium with 5% Fetal Bovine Serum (Hyclone), Serum Extender, 8 ng/ml 2.5S Nerve Growth Factor (Collaborative Research). The tissue was then incubated at 37°C in Earl's Balanced Salt Solution (EBSS) with 0.1% Collagenase, Type II (Sigma) for 30 min with gentle agitation every 10 min. Papain, 50 U/ml (Worthington Biochemical), was then added and the tissue was incubated at 37°C for an additional 30 min with gentle agitation every 10 min. The tissue was allowed to settle, the supernatant removed and the tissue was gently triturated in NCM with 0.5% Bovine Serum Albumin (BSA) using fire-polished Pasteur pipettes until most of the tissue was dissociated. The solution containing the dissociated cells was then underlayed with an equal volume of MEM with 4% BSA, centrifuged, resuspended in NCM and finally plated on poly-d-lysine coated 25 cm^2 tissue culture flasks (T25) and maintained in a humidified, 37°C, CO_2 incubator. Following 3 days in culture the antimitotic agent 5-fluoro-2′-deoxyuridine was added to inhibit non-neuronal cell proliferation. Neurons were maintained for 10–14 days prior to use in order to maximize the number of synaptic contacts within the culture. Due to the small amount of tissue obtained from each animal, 30 animals (60 nodose ganglia) were utilized to seed six T25 tissue culture flasks. Therefore, each flask contained pooled neurons equivalent to that from 5 animals (10 nodose ganglia), resulting in a plating density of approximately 1600 neurons/cm^2. Cell density was not significantly different from flask to flask. Each lane represents the contents of one T25 flask. A total of 137 T25 flasks were used in these experiments.

Protein Phosphorylation and Immunoprecipitation of Synapsin I

Assays were performed according to Nah et al. [22] with some modifications according to Fukunaga and colleagues [6]. Cells were washed three times with phosphate free DMEM. After 20 min at 37°C in the same medium, ^{32}P orthophosphate, carrier-free, (Amerisham, 0.15 mCi/ml final) was added and cells were incubated for 5 hr at 37°C, 5% CO_2, 95% O_2. Cells were then washed 2 times in $CaCl_2$-free Krebs-Ringers-HEPES buffer (KRH) (in mM): (128 NaCl, 5 KCl, 1 Na_2HPO_4, 1.2 $MgSO_4$, 10 Glucose and 20 HEPES). After 30 min in the same solution, the cells were incubated with metabotropic receptor ligands (Tocris Cooksin) in KRH with 2 mm $CaCl_2$ for 15 min followed by a 1 min depolarization with KCl, 60 mM final concentration. Control flasks received vehicle additions of KRH with 2 mm $CaCl_2$. All supernatant was then aspirated and cells were snap frozen using a dry ice/methanol bath. Cells were solubilized with the addition of 1 ml of solubilization buffer (0.5% SDS, 2.5% (vol/vol) Nonidet P-40, 150 mM NaCl, 35 mM NaF, 2 mM EGTA, 10 mM HEPES, 1 mg/ml Pefabloc, 10 μM Leupeptin, and 5 μg/ml A Protinin, pH 7.4). The mixture was then thawed and placed on a rocking tray for 5 min. Contents were transferred to a microcentrifuge tube and centrifuged at 14,000 × *g* for 15 min to remove insoluble material. The supernatant was transferred to a new tube, 4 μl of synapsin I IgG (Chemicon, 0.2 μg/μl) was added and the samples were incubated overnight at 4°C. Prewashwed protein A-Sepharose (30 μl packed beads/sample) in solubilization buffer was added and the samples were incubated for 4 hr at 4°C. The beads were washed three times with 1 ml solubilization buffer, suspended in Laemmli (2% SDS, 6 M urea, 62.5 mM Tris, pH 6.8) buffer and heated to 70°C for 5 min. The supernatant was subjected to SDS-PAGE using 4–20% Tris-HCl precast gels (Bio-Rad). The synapsin I band was identified by Coomassie staining and autoradiography. Each experiment shown was preformed at least three times using separate preparations.

For quantification of phosphate incorporation in synapsin I separated by electrophoresis, computer images of films were taken with a CCD camera. Individual bands in the images were quantified by using a computer program for image analysis (NIH Image, version 1.6). Band densities were within the linear range of the camera sensitivity. All measurements are normalized to a percentage of control, baseline synapsin I phosphorylation. Averaged data are presented in the text as means ± SE. The statistical significance of observed differences was determined using two-tailed Student's *t* tests, with $P < 0.05$ as minimal level of significance.

Due to the small amount of protein loaded in each lane, the absolute amount of protein was not determined. To compare relative levels of protein loaded in each lane, Coomassie Blue staining of the gels was performed and resulted in a single band between 80–86 kDal with similar levels of Coomassie Blue staining intensity in each lane (Fig. 2*E*).

Immunocytochemistry

For immunocytochemical localization of synapsin I in the visceral afferent neurons, cultured nodose neurons were fixed in 4% paraformaldehyde for 30 min and processed as follows: (i) rinsed in 0.1 M phosphate-buffered saline (PBS) for 30 min; (ii) permeabilized with 0.3% hydrogen peroxide for 30 min at room temperature; (iii) rinsed in 0.1 M PBS for 30 min; (iv) blocked with PBS with 3% normal goat serum and 0.25% triton X-100 (Sigma, St. Louis) for 2 hr; (v) rinsed in 0.1 M PBS three times; (vi) incubated in primary antibody for 24 hr at 4°C; (vii) rinsed three times in 0.1 M PBS; (viii) incubated with biotinylated

Table 1. Metabotropic glutamate receptor and control primer sets used for the PCR amplification of cDNAs

Gene	Primers		PCR product size
mGluR1[1]	Forward	5′ CCAGTGATGTTCTCCATACC 3′	361
	Reverse	5′ CACTCTGGGTAGACTTGAGTG 3′	
mGluR2[1]	Forward	5′ TTTAGGTCAGAAGCCAGAGT 3′	250
	Reverse	5′ CAGTAACCATCCTCTCTATCC 3′	
mGluR3[1]	Forward	5′ TATTCTCAGTCCTCTGCAAG 3′	261
	Reverse	5′ TTGTAGCACATCACTACATACC 3′	
mGluR4[1]	Forward	5′ TCATTTTCTCTTCTGTTCCC 3′	340
	Reverse	5′ GACATGCTACACATCAGAGAC 3′	
mGluR5[1]	Forward	5′ CCCCAAACTCTCCAGTCT 3′	210
	Reverse	5′ ATTTTTCACCTCGGGTTC 3′	
mGluR6[1]	Forward	5′ CAAGTAGCAAGGTTGAGTGT 3′	363
	Reverse	5′ GGTTGTAGTGTTGGATCAAG 3′	
mGluR7[1]	Forward	5′ GAACTCTGTGAAAATGTAGACC 3′	321
	Reverse	5′ TTAGGGAGTCCAGAATTACAG 3′	
mGluR8[1]	Forward	5′ CGAGGGTTATAACTACCAGGT 3′	440
	Reverse	5′ TAGGTGCTGTGACAGATTTCT 3′	
GAPDH	Forward	5′ CATAGACAAGATGGTGAAGGTCGG 3′	550
	Reverse	5′ GCCAAAGTTGTCATGGATGACC 3′	

[1] Similar to those previously published in Ghosh et al., 1997.

antirabbit immunoglobulin (IgG) for 2 hr; (ix) rinsed in 0.1 M PBS 3 times; (x) placed in Texas-Red Avidin D for 1 hr (Vector Laboratories); (xi) rinsed in 0.1 M PBS 3 times; (xii) dehydrated and coverslipped. Negative controls included omission of primary antibody and omission of secondary antibody. Slides were then imaged with fluorescent microscopy using a rhodamine filter cube set. Photomicrographs were obtained with a CCD camera. The sources and dilutions for the primary antibodies and antiserum used are as follows: rabbit anti-synapsin I (1:2000, Chemcon), biotinylated goat anti-rabbit IgG (1:200, Vector labs).

Patch-Clamp Techniques

All experiments were performed on isolated nodose neurons following 24–36 hr in culture. This relatively short culture period did not allow for extended neurite growth and ensured adequate space clamp. Whole-cell currents were recorded using perforated patch-clamp techniques with polished glass electrodes (1–3 MΩ resistance). Reference electrode was an Ag-AgCl plug immersed in a 150 mM KCl agar bridge that was placed in the bath. Recordings were made at room temperature using a Axopatch 1D patch clamp amplifier and filtered at 3 kHz using a 4-pole Bessel filter. Currents were digitized on line at 10 kHz and stored for analysis. Leak currents were determined by applying hyperpolarizing pulses from −80 to −90 mV. Linear scaling of the leak current observed at −90 mV resulted in less than a 1.8 pA leak current were peak Ca^{++} currents were measured (near 0 mV) and thus were not subtracted. Typical values for series resistance in the perforated patch with the solutions described below were 10–12 MΩ. Currents were analyzed using the Axograph data analysis program (Axon Instruments, Foster City, CA).

Solutions

To isolate calcium currents, the following solutions were used: Bath; (in mM): 140.0 tetraethylammonium (TEACl), 5.0 4-aminopyridine, 15.0 glucose, 10.0 HEPES, 2.0 $CaCl_2$, pH 7.38. Pipette; (in mM): 124.0 CsCl, 11.0 EGTA, 1.0 $CaCl_2$, 2.0 $MgCl_2$, 10.0 HEPES, and 258 U/ml nystatin, pH 7.3.

RT-PCR

From nodose neurons in culture as described above, mRNA was isolated using Dynal's mRNA Isolation Micro Kit as per manufacturer's protocol. First strand cDNA synthesis and PCR were performed using Stratagene's RT-PCR kit. First strand cDNA synthesis was performed as per the manufacturer's protocol. The PCR reaction was performed by mixing 5 μl of the cDNA template with 5 μl of 10× PCR buffer, 0.5 μl 100 mM dNTPs, and 20 pmol of each oligonucleotide primer in a thin-walled 0.2 μl PCR tube. The reaction was then brought up to 49.5 μl using DEPC-treated H_2O. Subsequent incubation at 90°C for 5 min then 54°C for 5 min was followed by the addition of 0.5 μl Taq polymerase into these reaction tubes.

The PCR reaction initiated with a denaturation step at 94°C (5 min). This was followed by 30 cycles at 95°C (15 sec), 52°C (1 min), and 72°C (2 min). The PCR reaction was terminated with a final step at 72°C (7 min). The PCR amplified products were electrophoresed on a 2.0% agarose gel and visualized with ethidium bromide staining. All mGluR and glyceraldehyde 3-phosphate dehydrogenase (GAPDH) primer sequences are listed in the Table.

Rat cerebellum, olfactory bulb and cerebral cortex served as positive controls for the mGluR primers due to each tissue's prominent expression of different mGluR subtypes. Cerebellum served as positive control tissue for mGluRs 1, 2 and 4 while the olfactory bulb prominently expresses mGluRs 6, 7 and 8. The cerebral cortex served as positive control tissue for mGluRs 3 and 5. Adult, male Sprague-Dawley rats were anesthetized with halothane and decapitated. Tissues of interest were removed then frozen under liquid nitrogen. mRNA isolation and subsequent RT-PCR were performed as described above. To confirm that the PCR reaction did not amplify genomic DNA,

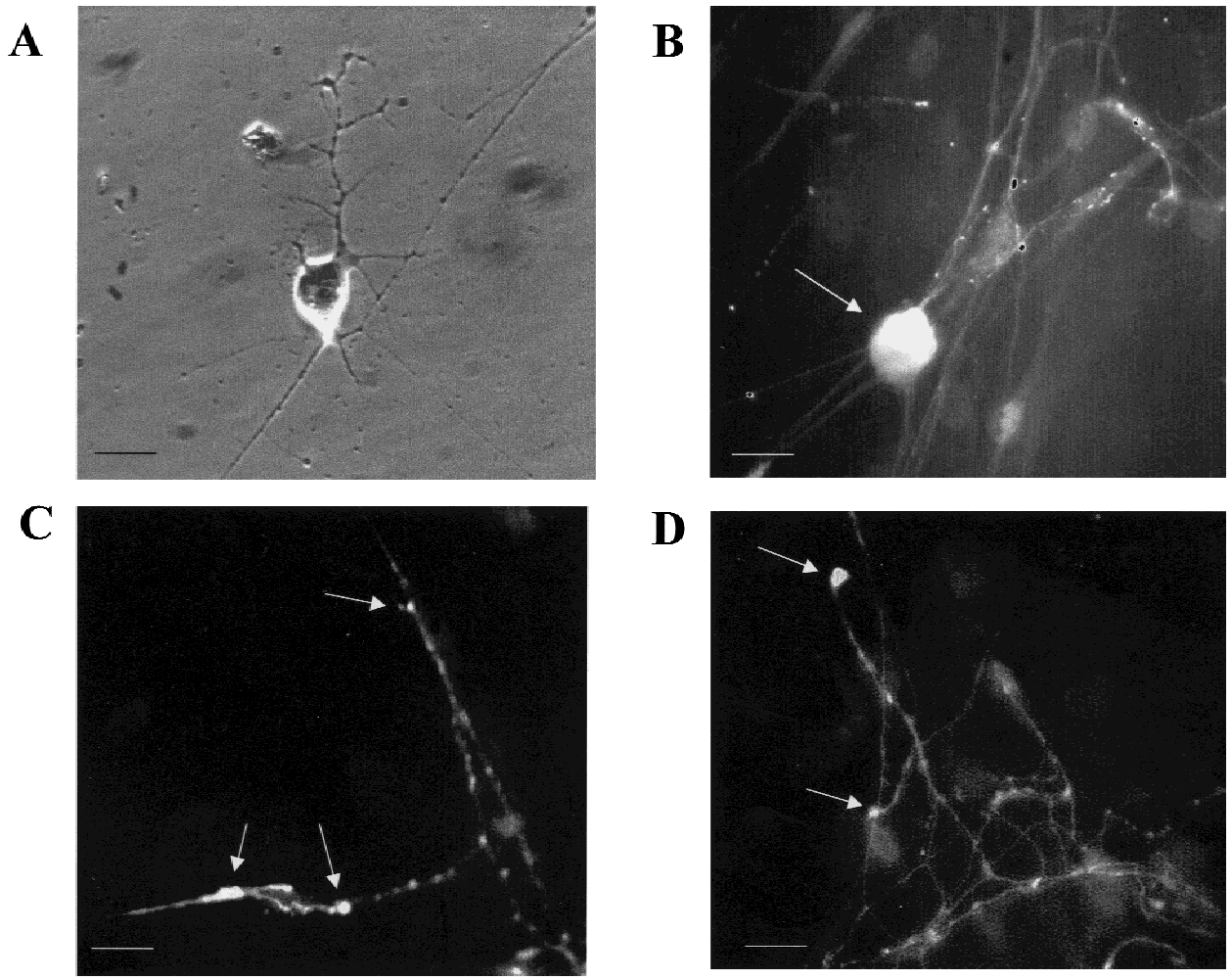

Fig. 1. (*A*) A brightfield micrograph of a nodose neuron following 14 days in culture. (*B*) Fluorescent illumination with a rhodamine filter revealing the presence of synapsin I immunoreactivity in the cell soma (white arrow). Bar = 30 μm. (*C* and *D*) Synapsin I immunoreactivity in processes and terminals of nodose neurons in culture. Bar = 5 μm.

mRNA underwent reverse transcriptase in the absence of MMLV-RT. Products from this reaction were then used in the PCR amplification of GAPDH. Evaluation of PCR products were performed as described above.

Results

Immunofluorescent Localization of Synapsin I in Nodose Ganglia Neurons

The expression of synapsin I in nodose ganglia neurons was evaluated using affinity-purified antibodies that specifically recognize synapsin I. Figure 1*A* is a bright-field photomicrograph of a nodose neuron in culture for 14 days. Figure 1*B–D* are fluorescent photomicrographs. Synapsin I immunoreactivity was present in nodose neuron soma (Fig. 1*B*), processes and terminals (Fig. 1*C* and *D*). Synapsin I immunoreactivity was observed in virtually all nodose neurons in the culture.

mGluR Agonist Inhibition of Voltage-Gated Calcium Channels

Phosphorylation of synapsin I is known to be increased by depolarization activation of voltage-gated calcium channels and the subsequent activation of Ca^{++}/calmodulin-dependent kinases [12]. If mGluR activation inhibits depolarization-induced synapsin I phosphorylation, this may be due to mGluR inhibition of voltage-gated Ca^{++} currents. Previous studies have shown that in

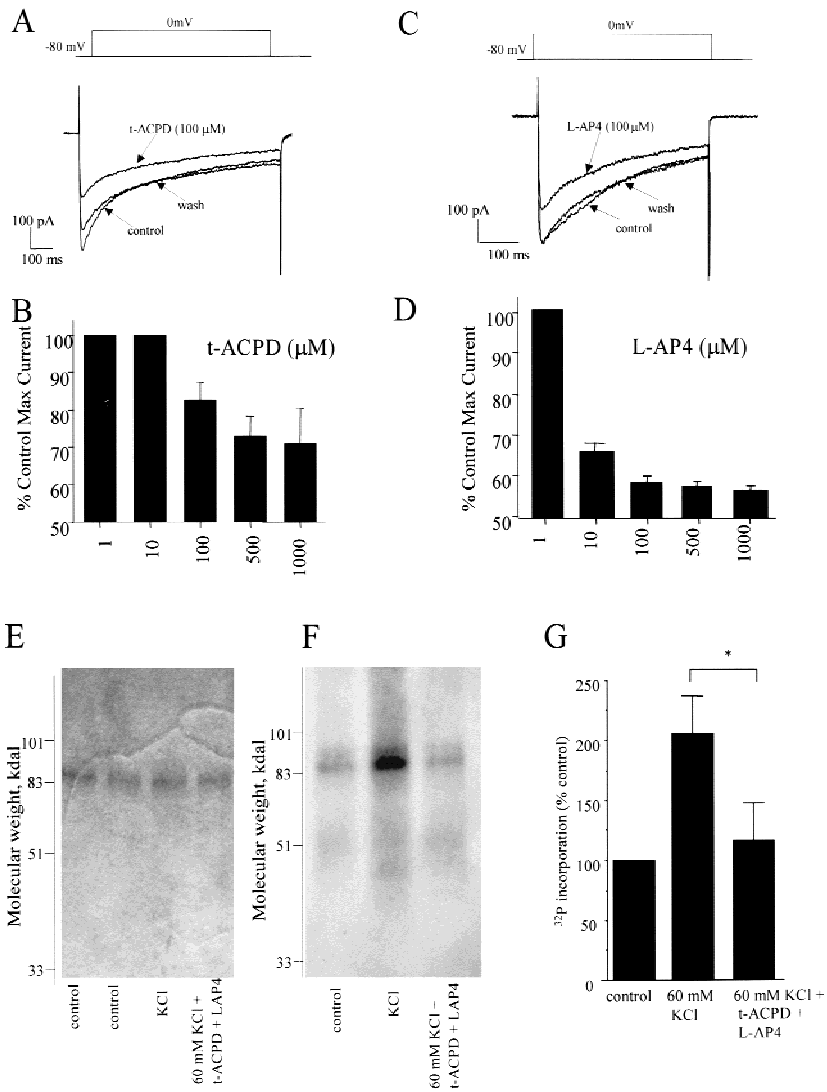

Fig. 2. (*A–D*) illustrate the inhibitory effects of t-ACPD and L-AP4 on nodose ganglia evoked calcium currents. (*A*) Calcium currents evoked by 0 mV step depolarizations from a −80 mV holding potential before, during and following exposure to 100 μM t-ACPD. (*B*) Averaged response (mean ± SEM) of evoked peak calcium current to varying concentrations of t-ACPD (1.0 μM, $n = 3$; 10.0 μM, $n = 4$; 100 μM, $n = 9$; 500 μM, $n = 8$; 1000 μM, $n = 5$). (*C*) Calcium currents evoked by 0 mV step depolarizations from a −80 mV holding potential before, during and following exposure to 100 μM L-AP4. (*D*) Averaged response (mean ± SEM) of evoked peak calcium current to varying concentrations of L-AP4 (1.0 μM, $n = 3$; 10.0 μM, $n = 9$; 100 μM, $n = 4$; 500 μM, $n = 4$; 1000 μM, $n = 4$). (*E*) Coomassie Blue stained gel illustrating the relative amounts of protein loaded in each lane. Similar results were obtained in all other gels stained. (*F*) Effects of 1.0 mM ACPD + 1.0 mM L-AP4 on high-K^+-induced phosphorylation of synapsin I. Molecular mass given in kDa. Shown is an autoradiogram from a 10-day exposure at −70°C. (*B*) Quantification of radioactive phosphate incorporation into synapsin I. Values represent mean ± SE percentage change from control phosphorylation ($n = 5$). * = $P < 0.05$.

visceral sensory neurons of the nodose ganglia the channel responsible for approximately 70% of the total Ca^{++} current has been shown to be a N-type, ω-conotoxin GVIA sensitive Ca^{++} channel [20]. In addition, we have previously reported that mGluRs partially inhibit the N-type calcium current in nodose ganglia neurons [16]. Figure 2*A–D* illustrate the dose-dependent effects of the broad spectrum mGluR agonist 1-amino-cyclopentane-1s-3r-dicarboxylic acid (t-ACPD, $n = 13$) and the mGluR group III agonist L(+)-2-amino-4-phosphonobutyric acid (L-AP4, $n = 8$) on evoked calcium currents in nodose ganglia neurons. Calcium currents were evoked by a step depolarization to 0 mV from a −80 mV holding potential. Application of 1 mM t-ACPD and 1 mM L-AP4 inhibited the calcium current evoked current by 29 ± 11% and 42 ± 3%, respectively.

mGluR Agonist Inhibition of Depolarization-Induced Synapsin I Phosphorylation

To determine if these same concentrations of t-ACPD and L-AP4 could also modulate depolarization-induced phosphorylation of synapsin I, we measured the incorporation of ^{32}P phosphate into synapsin I following KCl induced depolarization in the absence and presence of t-ACPD and L-AP4. Due to the nature of our preparation and the number of animals required for each experiment, dose-response relationships for the mGluR effects on synapsin I phosphorylation were not performed. Following immunoprecipitation, SDS-PAGE and autoradiography, radiolabeled synapsin I appeared as a band between 80 and 86 kilodaltons representing Ia and Ib isoforms. In most gels, we were unable to distinguish

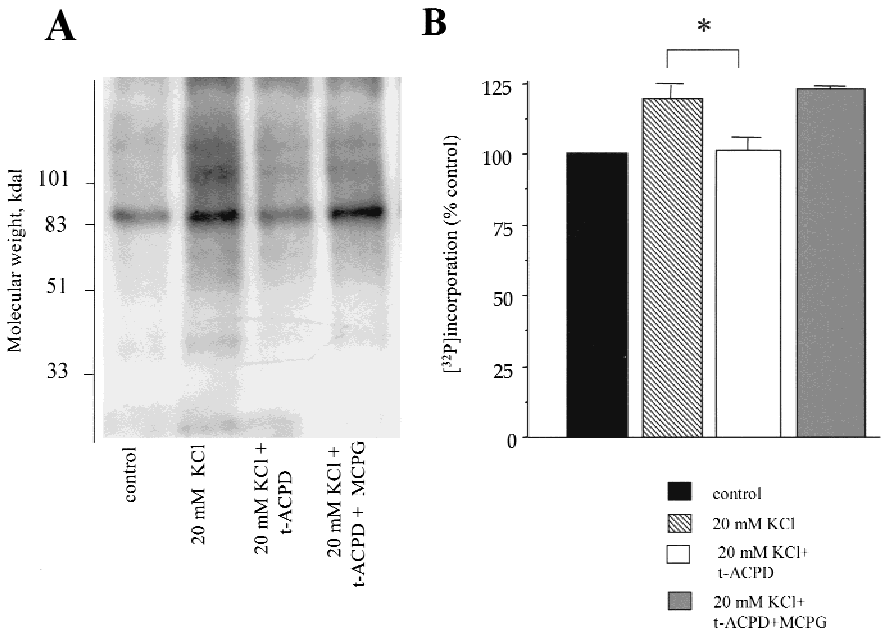

Fig. 3. (*A*) SDS-PAGE of phosphorylated synapsin I from nodose neurons illustrating the effects of 1.0 mM t-ACPD on 20 mM KCl induced phosphorylation of synapsin I in the absence and presence of MCPG. Molecular mass given in kDa. (*B*) Averaged effects of t-ACPD induced inhibition of 20 mM KCl induced phosphorylation of synapsin I and 1.0 mM MCPG blockade of this effect. Solid black bar = control; hatched bar = 20 mM KCl ($n = 6$); white bar = 10 mM KCl + 1.0 mM t-ACPD ($n = 3$), Solid gray bar = 20 mM KCl + 1.0 mM t-ACPD + 1.0 mM MCPG ($n = 3$); * = $P < 0.05$.

between the two isoforms of synapsin I. Depolarization of nodose neurons with 60 mM KCl increased phosphorylation of synapsin I relative to control by 104 ± 26% (Fig. 2*F* and *G*, $n = 5$). Following treatment of nodose neurons with a combination of mGluR agonists consisting of 1.0 mM t-ACPD and 1.0 mM L-AP4 for 15 min prior to KCl depolarization, depolarization increased synapsin I phosphorylation relative to control by only 10.0 ± 10%, which was not significantly different (Fig. 2*F* and *G*, $n = 5$). Coomassie Blue staining of the gels revealed no observable difference in relative amounts of protein in each lane (Fig. 2*E*).

Application of the broad spectrum mGluR antagonist (S)-α-Methyl-4-carboxyphenylglycine (1 mM MCPG) effectively blocked the inhibitory effects observed with t-ACPD (Fig. 3), but had no significant effect on the inhibitory response observed with L-AP4 (Fig. 4). Furthermore, application of (S)MCPG alone had no effect on resting levels of synapsin I phosphorylation ($n = 4$, *data not shown*).

Given that in some regions of the central nervous system activation of mGluRs can increase postsynaptic function and activate neurons [4], we examined the ability of mGluR agonists t-ACPD and L-AP4 to alter the phosphorylation state of synapsin in nodose neurons in the absence of KCl induced membrane depolarization. In the absence of KCl-induced depolarization, neither application of t-ACPD ($n = 8$) or L-AP4 ($n = 3$) alone altered baseline synapsin I phosphorylation relative to control (Fig. 5).

Identification of mGluR Receptor Expression in Nodose Neurons

Due to the extremely large number of animals that would be required to complete agonist-selective dose-response studies, we utilized RT-PCR methodology to identify the mGluR receptors expressed in nodose neurons. All mGluR primers were similar to those previously published [11].

Each mGluR primer was cycled in reaction tubes containing either experimental cDNA template or positive control cDNA template. Positive control cDNA template for mGluRs 1, 2 and 4 originated from mRNA isolated from the cerebellum. Positive control templates for mGluRs 3 and 5 originated from mRNA isolated from the cerebral cortex while positive control cDNA templates for mGluRs 6, 7 and 8 originated from mRNA isolated from the olfactory lobe. All tissue were isolated from adult, male S/D rats. To test if isolated mRNA samples contained genomic DNA contamination, experimental mRNA in the absence of RT was added to a PCR reaction tube containing a primer set for the

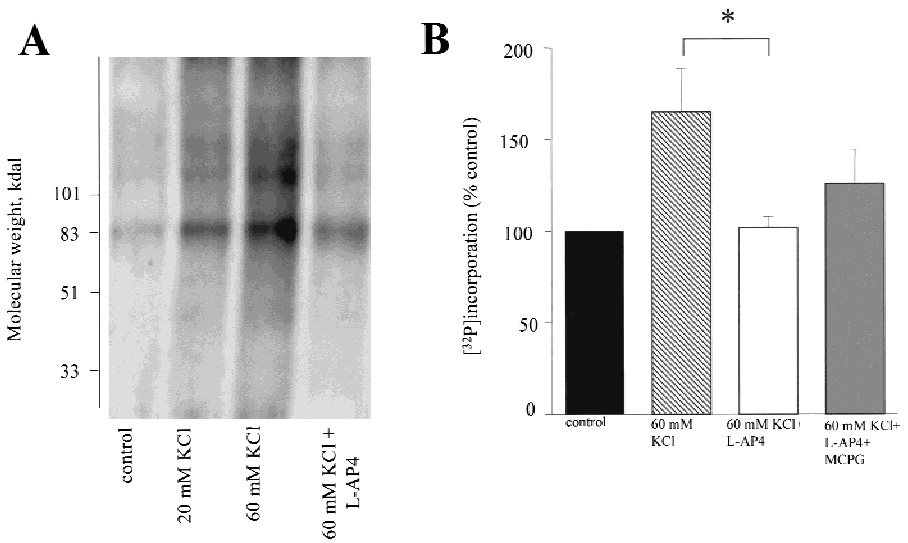

Fig. 4. (*A*) SDS-PAGE of phosphorylated synapsin I from nodose neurons illustrating the effects of 1.0 mM L-AP4 on 60 mM KCl induced phosphorylation of synapsin I. Molecular mass given in kDa. (*B*) Averaged effects of L-AP4 induced inhibition of 60 mM KCl-induced phosphorylation of synapsin I and the effect of 1.0 mM MCPG. Molecular mass given in kDa. Solid black bar = control; hatched bar = 60 mM KCl (n = 3); white bar = 60 mM KCl + 1.0 mM L-AP4 (n = 3), Solid gray bar = 60 mM KCl + 1.0 mM L-AP4 + 1.0 mM MCPG (n = 3); * = $P < 0.05$.

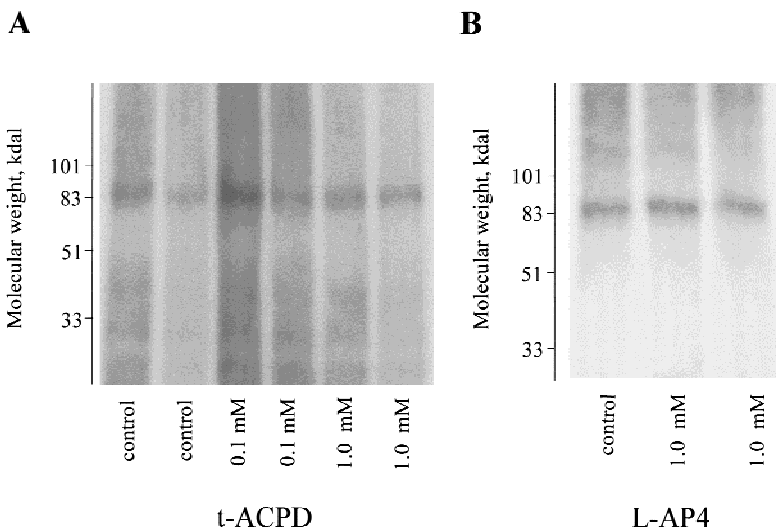

Fig. 5. (*A*) Effects of 1.0 and 0.1 mM t-ACPD on baseline phosphorylation of synapsin I. Similar results were obtained in 8 experiments. Molecular mass given in kDa. (*B*) Effects of 1.0 and 0.1 mM L-AP4 on baseline phosphorylation of synapsin I. Molecular mass given in kDa. Similar results were obtained in 3 experiments.

housekeeping gene GAPDH while another amplified the same primers only in the presence of experimental cDNA.

Using primers selective for group I and group II mGluRs, positive control PCR product was observed in isolated cerebellum tissue and no PCR product could be detected in nodose ganglia neurons for mGluR1, mGluR2, mGluR3 or mGluR5 (Fig. 6*A*). Likewise, no PCR product was detected for group III mGluR4 or mGluR6. However, primers for group III mGluR7 and mGluR8 revealed that nodose neurons strongly express mGluR7 and show light expression of mGluR8 (Fig. 6*B*). These results suggest that the mGluR subtypes responsible for inhibition of synapsin phosphorylation are most likely mGluR7 and mGluR8.

Discussion

Neurotransmitter exocytosis is known to be dependent on the influx of extracellular Ca^{++} [23, 24]. Neurotransmitter exocytosis is also known to involve a complex interaction among proteins that are associated with synaptic vesicles, some of which are modulated by protein kinase activation. Phosphorylation of synapsin I has

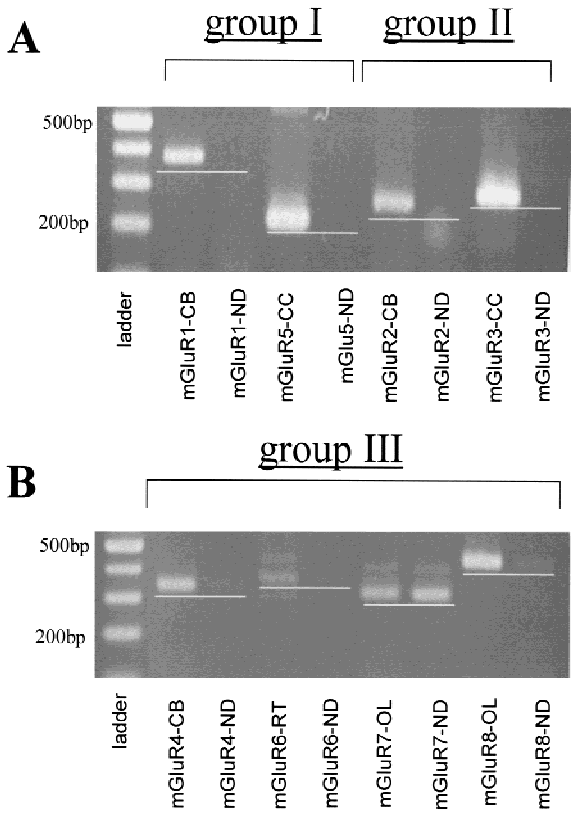

Fig. 6. RT-PCR analysis of mGluRs expressed in nodose ganglia. CB = cerebellum, ND = nodose ganglia, CC = cerebral cortex, OL = olfactory bulb. PCR products were visualized by ethidium bromide staining. Molecular size markers (in bp) are indicated on the right. (*A*) RT-PCR analysis of group I and group II mGluRs. Predicted PCR-products from the CB and CC for each mGluR are as follows: mGluR 1 at 361 bp, mGluR 5 at 210 bp, mGluR 2 at 250 bp, and mGluR 3 at 261 bp. The ND did not express any of these subtypes. (*B*) RT-PCR analysis of group III mGluRs. Predicted PCR-products from the CB and OL for each mGluR are as follows: mGluR 4 and 340 bp, mGluR 6 and 363 bp, mGluR 7 at 321 bp, and mGluR 8 at 440 bp. The ND expresses mGluRs 7 and 8.

been shown to be increased by depolarization induced Ca^{++} influx and the subsequent activation of Ca^{++}/calmodulin kinases in a number of different neuronal preparations [3]. It has been hypothesized that the regulation of neurotransmitter release is brought about by activation of intracellular second-messenger systems and consequent protein kinase activation. It is this cascade of events which ultimately may independently or interdependently modulate the function of both voltage-gated Ca^{++} channels and/or synaptic proteins. The ability of presynaptic mGluRs to modulate neurotransmitter release has been hypothesized to be due to mGluR inhibition of voltage-gated Ca^{++} channels as well as modulation of the phosphorylation of some synaptic vesicle-associated proteins [4]. Results from the present study suggest that phosphorylation of synapsin I can be regulated by agonists of mGluR receptors. Treatment of nodose ganglia neurons with mGluR agonists t-ACPD and L-AP4 reduces voltage-gated Ca^{++} currents and depolarization induced synapsin I phosphorylation. This result is consistent with our previous findings that application of mGluR agonists decrease in measured synaptic vesicle exocytosis in aortic baroreceptor neurons [15].

Metabotropic glutamate receptors (mGluRs) are a heterogeneous class of G-protein coupled receptors that have been found to be important in glutamatergic neurotransmission. At least 8 different subtypes have been characterized. Each of the subtypes has a distinct amino acid sequence, pharmacology, and signal transduction pathway [4, 24] and as a result, three major groups are recognized: Group I, which includes mGluR1 and mGluR5, is coupled to inositol triphosphate production and is activated by 3,5-dihydroxyphenylglycine (3,5-DHPG) and by the nonselective agonist (±)-1-Amino-cyclopentate-*trans*-1,3-dicarboxylic acid (t-ACPD); Group II, which includes mGluR2 and mGluR3, is activated (by 2S,1′R,2′R,3′R)-2-(2,3-dicarboxycyclopropyl) glycine (DCG-IV) and t-ACPD and are thought to be coupled to the inhibition of cAMP formation. Group III, which includes mGluR 4,6,7,8 is also coupled to the inhibition of cAMP and is selectively activated by L-2-Amino-4-phosphonobutyric acid (L-AP4) and also activated by higher concentrations of t-ACPD [27]. Both t-ACPD and L-AP4 were effective at attenuating depolarization induced synapsin I phosphorylation in the present study. However, the inhibitory effects of t-ACPD, but not L-AP4, were blocked by (S)MCPG. Furthermore, analysis of mGluR expression in these nodose ganglia neurons by RT-PCR suggests that only mGluR7 and mGluR8 are expressed in these cells. Thus, together, these data would suggest that mGluR7 and mGluR8 are involved in eliciting mGluR inhibition of synapsin I phosphorylation.

Under our test conditions, neither t-ACPD or L-AP4 had any effect on the phosphorylation of synapsin I under basal conditions. In addition, application of mGluR antagonist MCPG was without effect on baseline synapsin I phosphorylation. These results suggest that (i) the mechanisms governing resting synapsin I phosphorylation in nodose ganglia neurons may not be affected by mGluR activation; and (ii) there is no tonic, resting level of MCPG-sensitive mGluR activation altering synapsin I phosphorylation in these culture conditions. However, as described above, treatment with mGluR agonists does inhibit phosphorylation of synapsin I induced by depolarization. These results would suggest that in nodose ganglia neurons, the mechanisms underlying mGluR inhibition of synapsin I phosphorylation most likely involve interference with the transduction systems evoked by membrane depolarization and the subsequent Ca^{++}

signaling pathways required for increased synapsin I phosphorylation.

Perspectives

Visceral sensory afferents and baroreceptor afferents in particular, ascend centrally and synapse on medullary neurons within the nucleus of the solitary tract (NTS) where their combined information is integrated. Activity and time-dependent integration of this baroreceptor information is the first step in the normal regulation of cardiovascular reflex function. Alteration of the synaptic transmission between the baroreceptor afferents and NTS neurons has been suggested to contribute to inappropriate reflex control of sympathetic outflow. Although high-frequency stimulation of baroreceptor afferents has been shown to decrease evoked NTS excitatory potentials [2, 21] and results in a rightward shift in the baroreceptor reflex [1, 17], the cellular mechanisms underlying activity-dependent alterations in the signal transduction between baroreceptor afferents and NTS neurons are unknown. One potential mechanism that may be important in the modulation of baroreceptor afferent synaptic efficacy is an alteration in transmitter release from the presynaptic terminal. It has been suggested that the maintenance of synaptic transmission over a wide range of frequency stimulations requires that nerve terminals maintain pools of synaptic vesicles in reserve which can be recruited to active zones during periods of intense activity [23, 25, 26]. Thus, the mechanisms governing synaptic turnover at the baroreceptor terminals may serve as a common site for the regulation of baroreflex function. In the case of the baroreceptor/NTS synapses, failure to recruit vesicles to the baroreceptor exocytosis zones during periods of high activity could reasonably be hypothesized to lead to decreased synaptic efficacy, decreased NTS postsynaptic activation and ultimately allowing an increase in sympathetic outflow. Metabotropic glutamate receptors are known to play an important role in the regulation of neurotransmitter function at the level of the NTS [5, 8, 9, 10, 19]. Vesicle exocytosis is known to be regulated by calcium influx dependent second messenger systems and the phosphorylation and dephosphorylation of synaptic terminal associated proteins. Results from the present study may offer a mechanism by which activation of mGluRs on presynaptic baroreceptor afferents may inhibit synaptic transmission. The working hypothesis is that mGluR activation inhibits depolarization induced phosphorylation of synapsin I, thus decreasing the availability of synaptic vesicles from the reserve pool. This inhibition may be involved in the inhibition of transmitter release from baroreceptor afferent terminals during high frequency stimulation. Future studies will determine if other synaptic proteins are also modulated by mGluR activation and if these effects are involved in frequency dependent suppression of baroreceptor/NTS synaptic function.

The authors would like to thank Kathy Lindsley for her work on the immunoprecipitation experiments and her expert technical assistance. The authors would also like to thank Drs. Kevin Gillis and Calvin Hale for their critical reading of this manuscript.

References

1. Andresen, M.C., Kunze, D.L. 1994. Nucleus tractus solitarius-gateway to neural circulatory control. *Annu. Rev. Physiol.* **56:**93–116
2. Andresen, M.C., Yang, M. 1995. Dynamics of sensory afferent synaptic transmission in aortic baroreceptor regions of nucleus tractus solitarius. *J. Neurophysiol.* **74:**1518–1528
3. Ceccaldi, P.E., Grohovaz, F., Benfenati, F., Chieregatti, E., Greengard, P., Valtorta, F. 1995. Dephosphorylated synapsin I anchors synaptic vesicles to actin cytoskeleton: an analysis by videomicroscopy. *J. Cell Biol.* **128:**905–912
4. Conn, P.J., Pin, J.P. 1997. Pharmacology and functions of metabotropic glutamate receptors. *Annu. Rev. Pharm. Tox.* **37:**205–237
5. Foley, C.M., Moffit, J.A., Hay, M., Hasser, E.M. 1998. Glutamate in the nucleus of the solitary tract activates both ionotropic and metabotropic glutamate receptors. *Am. J. Physiol.* **275:**R1858–R1866
6. Fukunaga, K., Muller, D., Miyamoto, E. 1995. Increased phosphorylation of Ca^{2+}/calmodulin-dependent protein kinase 2 and its endogenous substrates in the induction of long-term potentiation. *J. Biol. Chem.* **270:**6119–6124
7. Gereau, R.W., Conn, P.J. 1995. Multiple presynaptic metabotropic glutamate receptors modulate excitatory and inhibitory synaptic transmission in hippocampal area CA1. *J. Neuroscience* **15:**6879–6889
8. Glaum, R.R., Miller, R.J. 1992. Metabotropic glutamate receptors mediate excitatory transmission in the nucleus of the solitary tract. *J. Neuroscience* **12:**2251–2258
9. Glaum, S.R., Miller, R.J. 1994. Inhibition of phosphoprotein phosphatases blocks metabotropic glutamate receptor effects in the rat nucleus tractus solitarii. *Mol. Pharmacol.* **45:**1221–1226
10. Glaum, S.R., Sunter, D.C., Udvarhelyi, P.M., Watkins, J.C., Miller, R.J. 1993. The actions of phenylglycine derived metabotropic glutamate receptor antagonists on multiple (1S,3R)-ACPD responses in the rat nucleus of the tractus solitarius. *Neuropharm.* **32(12):**1419–1425
11. Ghosh, P.K., Baskaran, N., van den Pol, A.N. 1997. Developmentally regulated gene expression of all eight metabotropic glutamate receptors in hypothalamic suprachiasmatic and arcuate nuclei-a PCR analysis. *Dev. Brain Res.* **102:**1–12
12. Greengard, P., Benfenati, F., Valtorta, F. 1994. Synapsin I, an actin-binding protein regulating synaptic vesicle traffic in the nerve terminal. *Advances in Second Messenger and Phosphoprotein Research* **29:**31–45
13. Greengard, P.,, Valtorta, F., Czernik, A.J., Benfenati, F. 1993. Synaptic vesicle phosphoproteins and regulation of synaptic function. *Science* **259:**780–785
14. Han, H.-Q., Greengard, P. 1994. Remodeling of cytoskeletal architecture of nonneural cells induced by synapsin. *Proc. Natl. Acad. Sci. USA* **91:**8557–8561
15. Hay, M., Hasser, E.M. 1998. Measurement of synaptic vesicle

exocytosis in aortic baroreceptor neurons. *Am. J. Physiol.* **275:** H710–H716
16. Hay, M., Kunze, D.L. 1994. Glutamate metabotropic receptor inhibition of voltage-gated calcium currents in visceral sensory neurons. *J. Neurophysiol.* **72:**421–430
17. Hayward, L.F., Hay, M., Felder, R.B. 1993. Acute resetting of the carotid sinus baroreflex by aortic depressor nerve stimulation. *Am. J. Physiol.* **264:**H1215–H1222
18. Jahn, R., Sudhof, T.C. 1994. Synaptic vesicles and exocytosis. *Annu. Rev. Neurosci.* **17:**219–246
19. Liu, Z., Chen, C.Y., Bonham, A.C. 1998. Metabotropic glutamate receptors depress vagal and aortic baroreceptor signal transmission in the NTS. *Am. J. Physiol.* **275:**H1682–H1694
20. Mendelowitz, D., Kunze, D.L. 1992. Characterization of calcium currents in aortic baroreceptors. *J. Neurophysiol.* **68:**509–517
21. Miles, R. 1986. Frequency dependence of synaptic transmission in nucleus of the solitary tract. *J. Neurophysiol.* **55:**1076–1090
22. Nah, S.Y., Saya, D., Barg, J., Vogel, Z. 1993. Opiate receptor agonists regulate phosphorylation of synapsin I in cocultures of rat spinal cord and dorsal root ganglion. *Proc. Natl. Acad. Sci. USA* **90:**4052–4056
23. Pieribone, V.A., Shupliakov, O., Brodin, L., Hilfiker-Rothenfluh, S., Czernik, A.J., Greengard, P. 1995. Distinct pools of synaptic vesicles in neurotransmitter release. *Letters to Nature* **375:**493–497
24. Pin, J.P., Duvoisin, R. 1995. The metabotropic glutamate receptors: Structure and functions. *Neuropharm.* **34:**1–26
25. Rothman, J.E. 1994. Intracellular membrane fusion. *In*: Molecular and Cellular Mechanisms of Neurotransmitter Release. L.P. Stjarne, S. Greengard, S. Grillner, T. Hokfelt, and D. Ottoson, editors. pp. 81–96. New York, Raven Press
26. Ryan, T.A., Smith, S.J. 1995. Vesicle pool mobilization during action potential firing at hippocampal synapses. *Neuron* **14:**983–989
27. Saugstad, J.A., Kinzie, J.M., Shinohara, M.M., Segerson, T.P., Westbrook, G.L. 1997. Cloning and expression of rat metabotropic glutamate receptor 8 reveals a distinct pharmacological profile. *Molecular Pharm.* **51:**19–125
28. Sollner, T., Rothman, J.E. 1994. Neurotransmission: harnessing fusion machinery at the synapse. *Trends in Neurosci.* **17:**344–347
29. Valtorta, F., Benfenati, F., Greengard, P. 1992. Structure and function of the synapsins. *J. Biol. Chem.* **267:**7195–7198